Yonekura, Terrisse, Alves Costa Silva et al. Cancer induces a stress ileopathy depending on β-adrenergic receptors and promoting dysbiosis that contribute to carcinogenesis.

Supplemental Figure legends

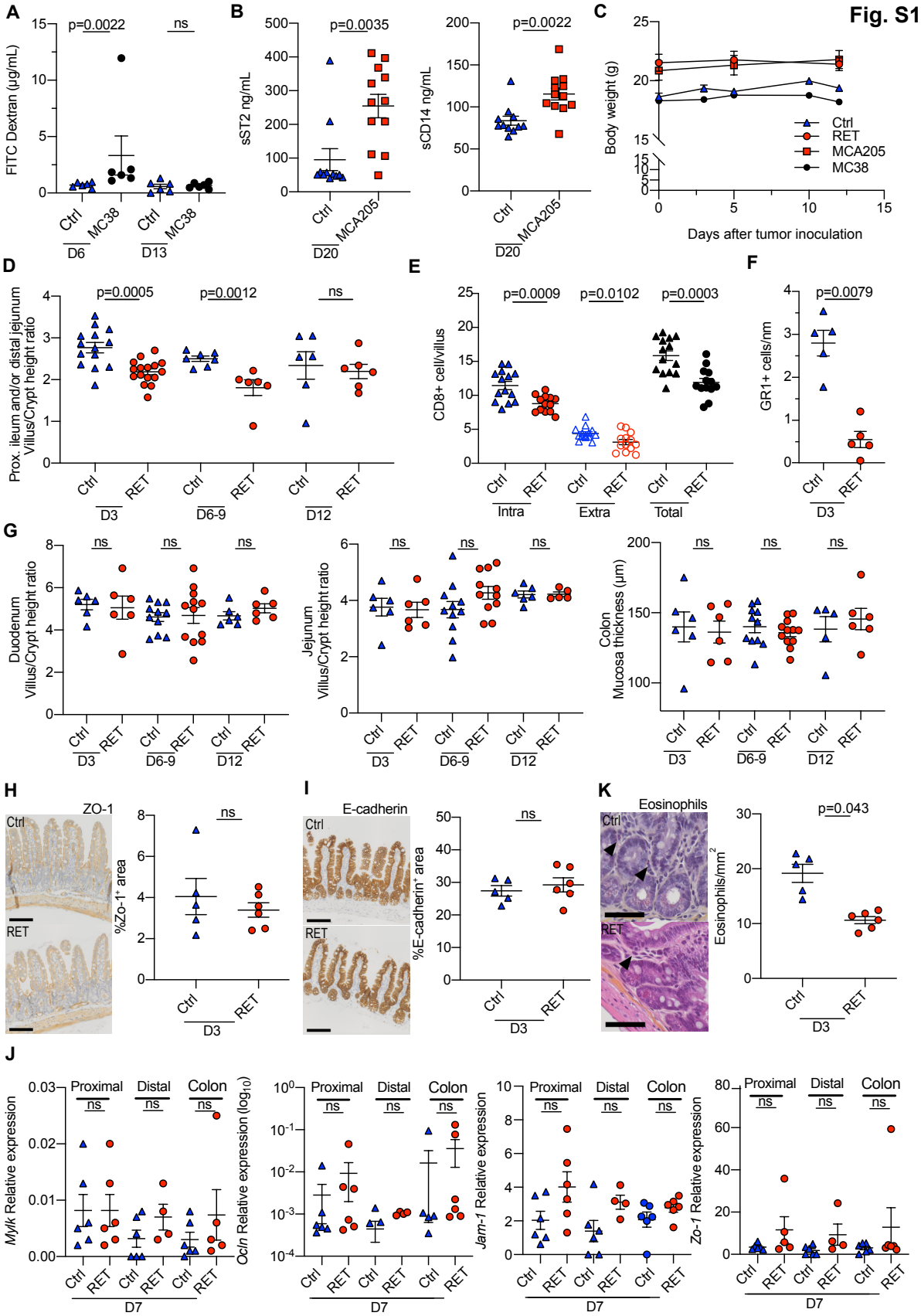

Supplemental Figure 1. Morphological abnormalities associated with cancer-induced ileopathy.

A. MC38-induced intestinal permeability monitored by FITC dextran oral administration at day 6 (left) and 13 (right) and translocation in the blood stream 4 hr later. Each dot represents one mouse. **B**. Plasma levels of soluble CD14 and ST2 at day 20 in naive *versus* MCA205 sarcoma bearers. Two concatenated experiments are plotted. Each dot represents one mouse. **C.** Longitudinal body weight monitoring of naive and tumor bearers in three independent tumor models (RET, MC38, MCA205) in a representative experiment. Mean body weight for 5-6 mice/group is shown. **D.** Manual calculation of the villus/crypt height ratio in the proximal ileum and/ or distal jejunum of control and tumor bearers at different time points after RET melanoma subcutaneous injection. **E-F**. Quantification of ileal mucosa (total), intra- and extra-vascular- $CD8^+$ lymphocytes (E) and granulocytes (F) by immunohistochemistry staining using anti- CD8, anti-Gr1 antibodies at 3 days after tumor injection. Numerical p values are indicated for Mann-Whitney test, ns: not significant. **G**. Manual calculation of the villus/crypt height ratio in the duodenum (left) and jejunum (middle) and mucosa thickness in colon (right) at 3 days, 6-9 days, 12 days after RET melanoma subcutaneous injection**. H-I.** Expression of tight junction molecule zonula occludens 1 (ZO-1) (G) and cell adhesion molecule E-cadherin (H) in the ileum by immunohistochemistry. Representative images of Zo-1 staining (left) and quantification of % of positive areas (right) in distal ileum of naive mice (n=5) and RET-bearing mice (n=6). Scale bars equal 100 µm. Symbols represent individual mice. Mann-Whitney test. **J.** Gene expression of tight junction molecules (*Zo-1*, *Ocln*, *Jam-1*, *Mylk*) in the ileum (proximal and distal) and colon tissue. at 6 days after tumor subcutaneous injection. Expression of each gene was normalized by *Ppia* expression. Symbols represent individual mice. Mann-Whitney test. **K.** Eosinophils counts/mm^2 in the ileum of naive *versus* RET-bearing mice 3 days after RET injection. Eosinophil morphology (left, black arrows) and quantification (right panel). Scale bar equals 50 µm. Each dot represents an individual mouse. *Numerical p values are indicated* for Mann-Whitney test.

Yonekura, Terrisse, Alves Costa Silva et al. Cancer induces a stress ileopathy depending on β-adrenergic receptors and promoting dysbiosis that contribute to carcinogenesis.

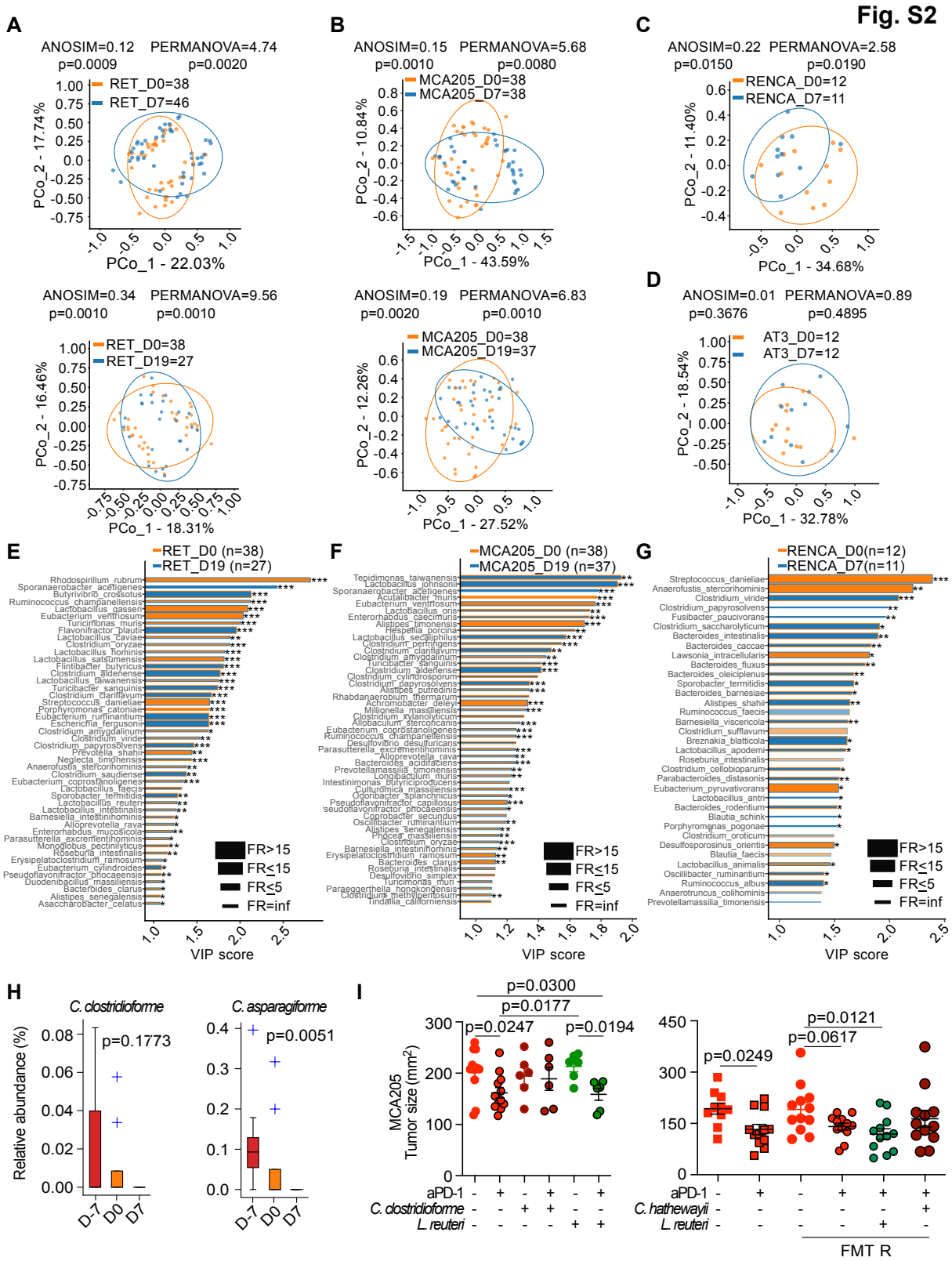

Supplemental Figure 2. Serial metagenomics analyses of stools from mice bearing a variety of different transplantable tumors.

A-B. Principal coordinate analysis of the taxonomic composition of feces in paired animals before (D0, orange dots, upper panel), 6-8 days after (D7, blue dots, upper panel), 19 days (D19, blue dots, lower panel) RET inoculation (A) or MCA205 (B) tumor bearing mice. **C-D.** Principal coordinate analysis of the taxonomic composition of feces in paired animals before (D0, orange dots), and 6-8 days after inoculation (D7, blue dots), RENCA (C), or AT3 (D) tumors. ANOSIM and PERMANOVA define the separation of the groups; p values define the significance of group separation after 999 permutations of the samples. **E-H**. Using Partial Least Square Discriminant Analysis (PLS-DA), coupled to a pair-wise comparison of relative taxonomic abundances (for species having a prevalence equal or greater than 5%), we analyzed taxonomic composition differences between the groups. Bar plot of fecal species that discriminate between pre- and post-tumor inoculation in mice, ordered by their VIP (variable importance) score. For each species, the bar color depicts the cohort with the highest mean relative abundance for a defined species, while the border color indicates the cohort with the lowest mean relative abundance. An absent border indicates mean relative abundance of zero in comparator cohort(s). *$p<0.05$, **$p<0.01$, *** $p<0.001$. The relative abundance of distinct OTUs is depicted in the three groups treated or not with vancomycin (H); Mann-Whitney test was used: *Numerical p values are indicated*. Bar thickness reports the FR value of the mean relative abundances for each species among the two cohorts. **I.** Cause-effect relationship between distinct Clostridia spp. and reduction of tumor immunosurveillance. Animals were treated with vancomycin for 7 days (D0 up to Day 7) and then fed with 10^9cfu of *Clostridium clostridioforme* or *Lactobacillus reuteri* before each ip administration of anti-PD-1 Ab every other 3 days for 4 injections (left panel). Fecal microbial transplantation (right panel) from a kidney cancer patient responding to nivolumab-based therapy was performed into an ATB-treated avatar mice that was then inoculated with RET and orally gavaged with109 cfu of *Clostridium hathewayi* or *Lactobacillus reuteri* before each i.p. administration of anti-PD-1 Ab every other 3 days for 4 injections. RET was inoculated s.c. at day 3 (I, left panel) or day 17 (I, right panel) and was followed bi-weekly by a caliper. Tumor sizes at sacrifice are depicted, each dot representing one animal. One representative experiment out of two yielding similar results is shown (I, right panel). Mann-Whitney test was used: *Numerical p values are indicated.*

Fig. S3

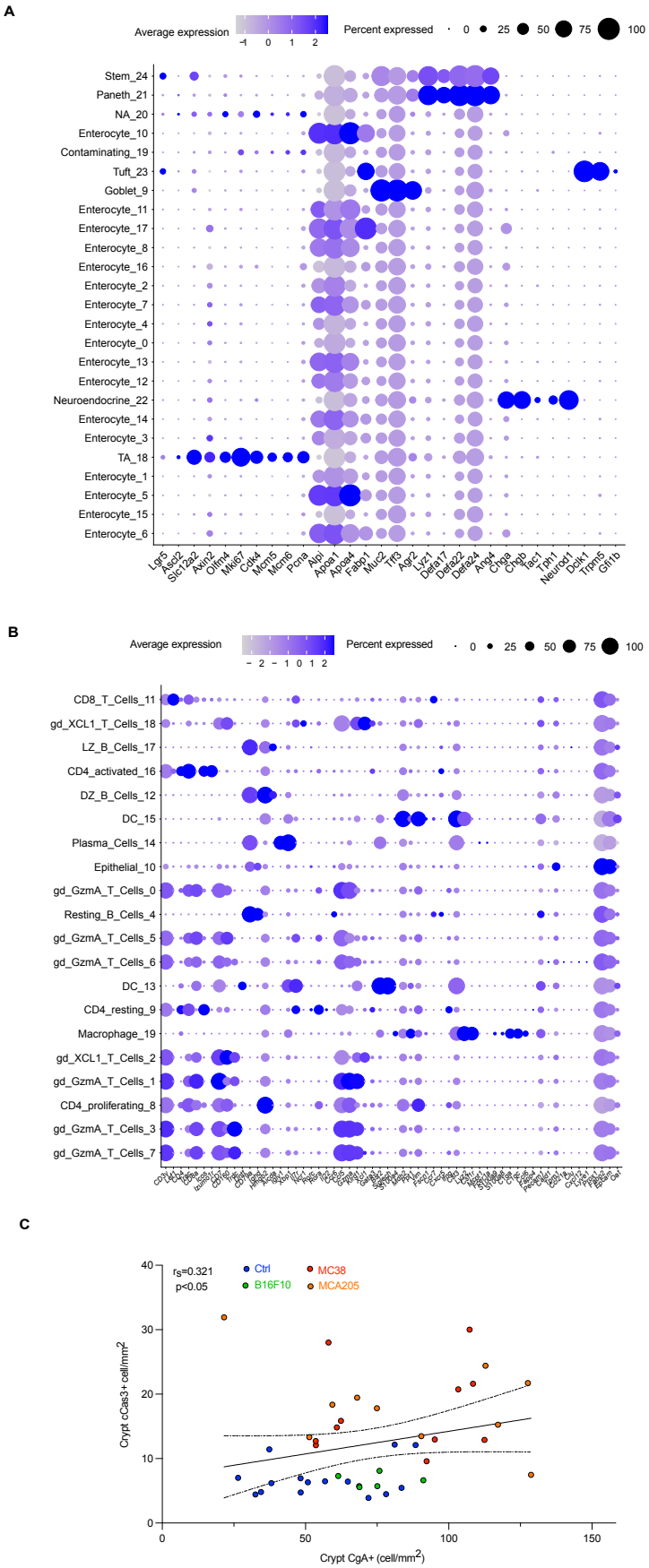
A
Average expression
Percent expressed
Stem_24
Paneth_21
NA_20
Enterocyte_10
Contaminating_19
Tuft_23
Goblet_9
Enterocyte_11
Enterocyte_17
Enterocyte_8
Enterocyte_16
Enterocyte_2
Enterocyte_7
Enterocyte_4
Enterocyte_0
Enterocyte_13
Enterocyte_12
Neuroendocrine_22
Enterocyte_14
Enterocyte_3
TA_18
Enterocyte_1
Enterocyte_5
Enterocyte_15
Enterocyte_6
Lgr5
Ascl2
Slc12a2
Axin2
Olfm4
Mki67
Cdk4
Mcm5
Mcm6
Pcna
Alpi
Apoa1
Apoa4
Fabp1
Muc2
Tff3
Agr2
Lyz1
Defa17
Defa22
Defa24
Arg4
Chga
Chgb
Tac1
Tph1
Neurod1
Dclk1
Trpm5
Gfi1b
B
Average expression
Percent expressed
CD8_T_Cells_11
gd_XCL1_T_Cells_18
LZ_B_Cells_17
CD4_activated_16
DZ_B_Cells_12
DC_15
Plasma_Cells_14
Epithelial_10
gd_GzmA_T_Cells_0
Resting_B_Cells_4
gd_GzmA_T_Cells_5
gd_GzmA_T_Cells_6
DC_13
CD4_resting_9
Macrophage_19
gd_XCL1_T_Cells_2
gd_GzmA_T_Cells_1
CD4_proliferating_8
gd_GzmA_T_Cells_3
gd_GzmA_T_Cells_7
C
rs=0.321
p<0.05
Ctrl
B16F10
MC38
MCA205
Crypt cCas3+ cell/mm2
Crypt CgA+ (cell/mm2)

Supplemental Figure 3. Dissection of cellular clusters in the ileal single cell transcriptomics analyses post-tumor implantation.

A-B. Identification and characterization of intestinal cell types in plate-based full-length single-cell RNA-seq data by unsupervised clustering related to Figure 3A. Post-hoc cluster annotation by the expression of known cell type markers (13) **A,B**. Dot plot showing average expression of consensus gene signature for epithelial cells clusters (A) or immune cells (B). Dot size represent the percentage of cells expressing a given gene (columns) within clusters (rows) and color code indicate mean gene expression (log_2(TPM+1)) within the cluster. **C.** Spearman correlation between CgA+ and cCasp3 across all tumor models. Idem as Figure 4b (right panel) but gathering the data from ten different experiments ran into C57BL/6 mice bearing day 7 established colon cancers, sarcoma or melanoma. Each dot represents one mouse/ileum. *Numerical p values are indicated.*

Yonekura, Terrisse, Alves Costa Silva et al. Cancer induces a stress ileopathy depending on β-adrenergic receptors and promoting dysbiosis that contribute to carcinogenesis.

Fig. S4

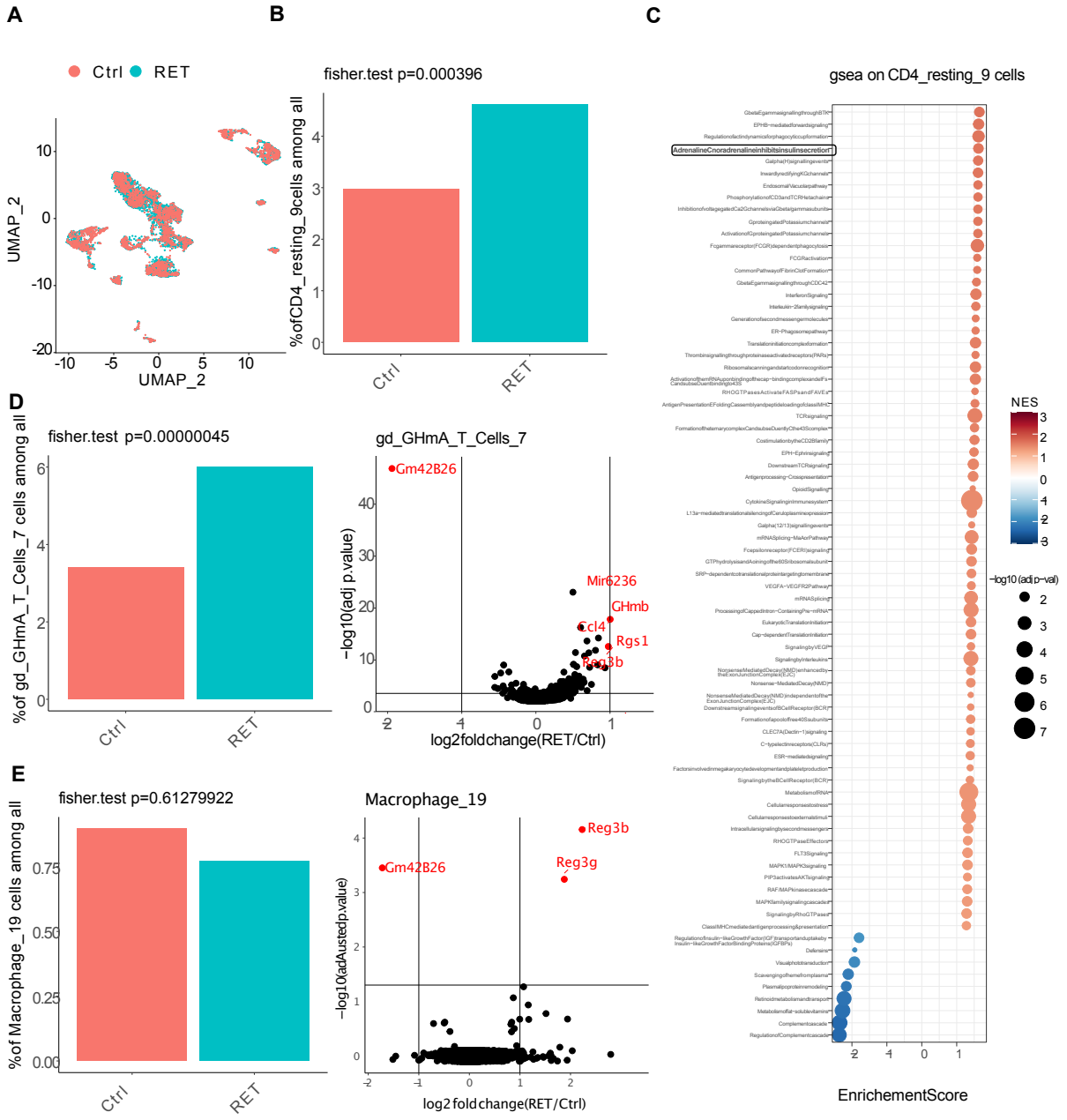

Supplemental Figure 4. Single cell transcriptomics analyses of ileal leukocytes post-tumor implantation.

A. Characterization of intestinal leukocytic cell types in plate-based full-length single-cell RNA-seq data by unsupervised clustering related to Figure 3A, overlaying PBS *versus* RET inoculated mice at 24 hrs. **B-C.** Relative proportions of CD4 cluster 9 (B) and dot plot of reactome database significantly enriched pathways in cluster 9. Dot sizes represent the log10(Q-value) determined by gene set enrichment analysis and color code indicates the normalized enrichment score. **D-E.** Relative proportions of Grzm A+ γδT cells from cluster 7 or macrophages (cluster 19) (refer to Fig. S3B) within ileal leukocytes in the 2 groups of animals (left panels). Volcano plots of differential gene expression patterns associated with a specific cell type segregating naive *versus* RET tumor bearers at 24 hours post RET implantation, according to Log2 p values and fold ratios for the proportion of each subtypes within the distal ileum for 3 animals/group (right panels). Significant differences are annotated in red. Statistics: Fisher exact test (bar graphs) and ANOVA (Volcano plots).

Yonekura, Terrisse, Alves Costa Silva et al. Cancer induces a stress ileopathy depending on β-adrenergic receptors and promoting dysbiosis that contribute to carcinogenesis.

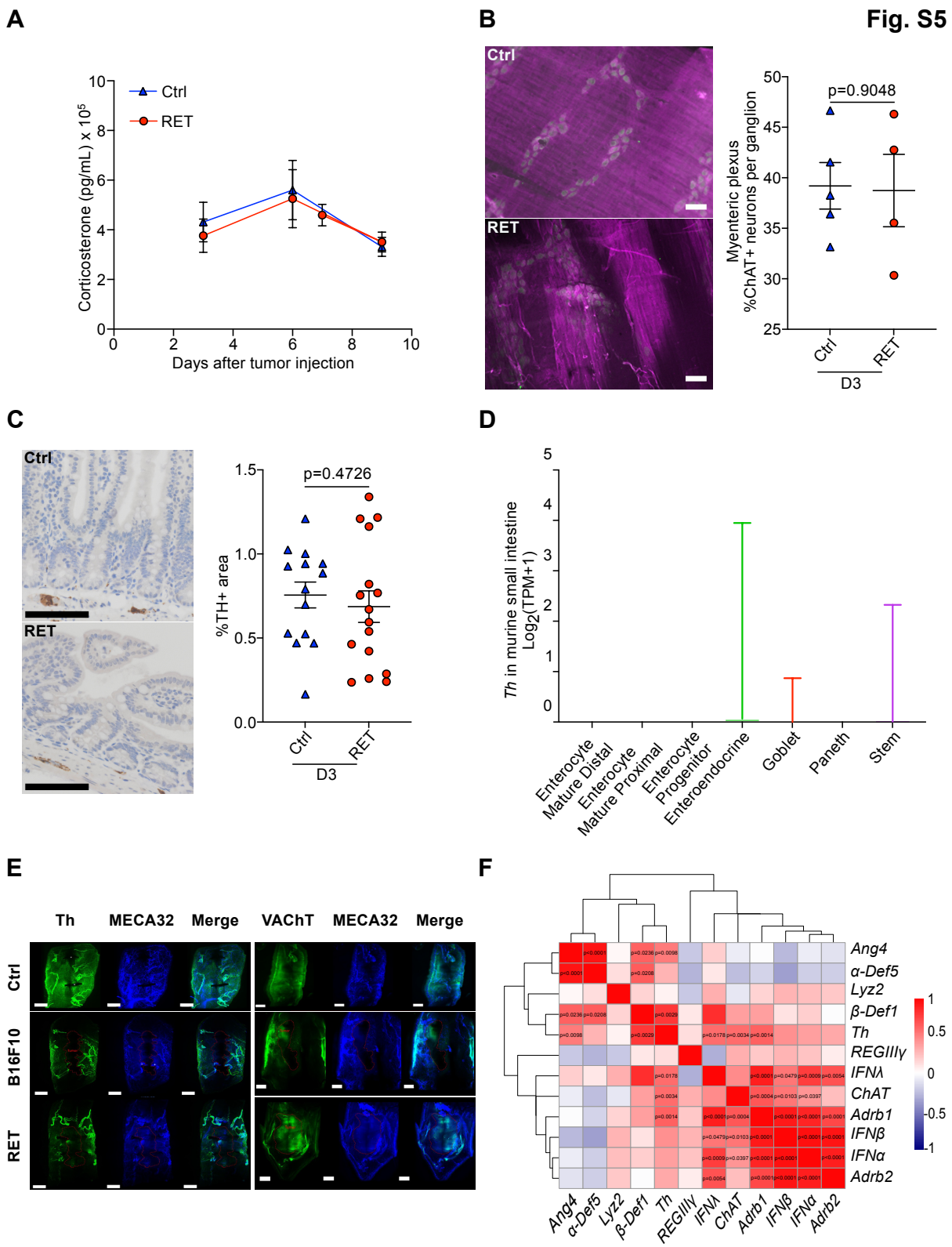

Supplemental Figure 5. Monitoring serum glucocorticoids and ChAT/TH balance in submucosae and myenteric plexus of ilea.

A. Kinetics study by ELISA measurements of corticosterone levels in plasma of RET tumor bearers and naive animals. Mean ±SEM for 6-9 animals/group is depicted in a representative experiment. **B**. Quantification of $ChAT^+$ neurons in the myenteric plexus of naive and RET tumor-bearing mice at 3 days after subcutaneous tumor inoculation using antibodies against ChAT (purple) and Hu (green). Four to five animals were examined by 2 independent researchers at day 3 post-tumor inoculation. Representative images of $ChAT^+$ staining (left) and quantification of % of $ChAT^+$ neurons per ganglion (right). Scale bars equal 50 µm. Symbols represent individual mice. *Numerical p values are indicated for* Mann-Whitney test. **C**. TH staining in the ileum (submucosa and myenteric plexus) of RET tumor bearers or naive animals at day 3 (C, left). Scale bars, 100 µm. Quantification of TH^+ area in all areas of ileum of RET tumor bearers or naive animals at day 3 (C, right). **D**. Expression of TH by EEC and other cell types according to publicly available data base reporting cluster-associated expression of distinct gene product by single cell RNA Sequence of naïve murine small intestinal cells (13). **E**. Visualization of melanoma innervation in the skin by immunofluorescence. TH (left pictures) and VaChT (right pictures) -specific staining as well as use of the pan-endothelial cell marker MECA32 to analyze vessels around the subcutaneous tumor (RET or B16F10 melanoma) 7 days after tumor subcutaneous inoculation. Scale bar equals 1.5 mm. A representative photograph is shown for each tumor and staining. **F.** Heatmap of correlation matrix of gene expression with non-supervised hierarchical clustering. Paneth cell-related gene product relative quantification using quantitative RT-PCR at day 3 after RET inoculation. Red to blue gradient for Spearman's rho. *Numerical p values are indicated.*

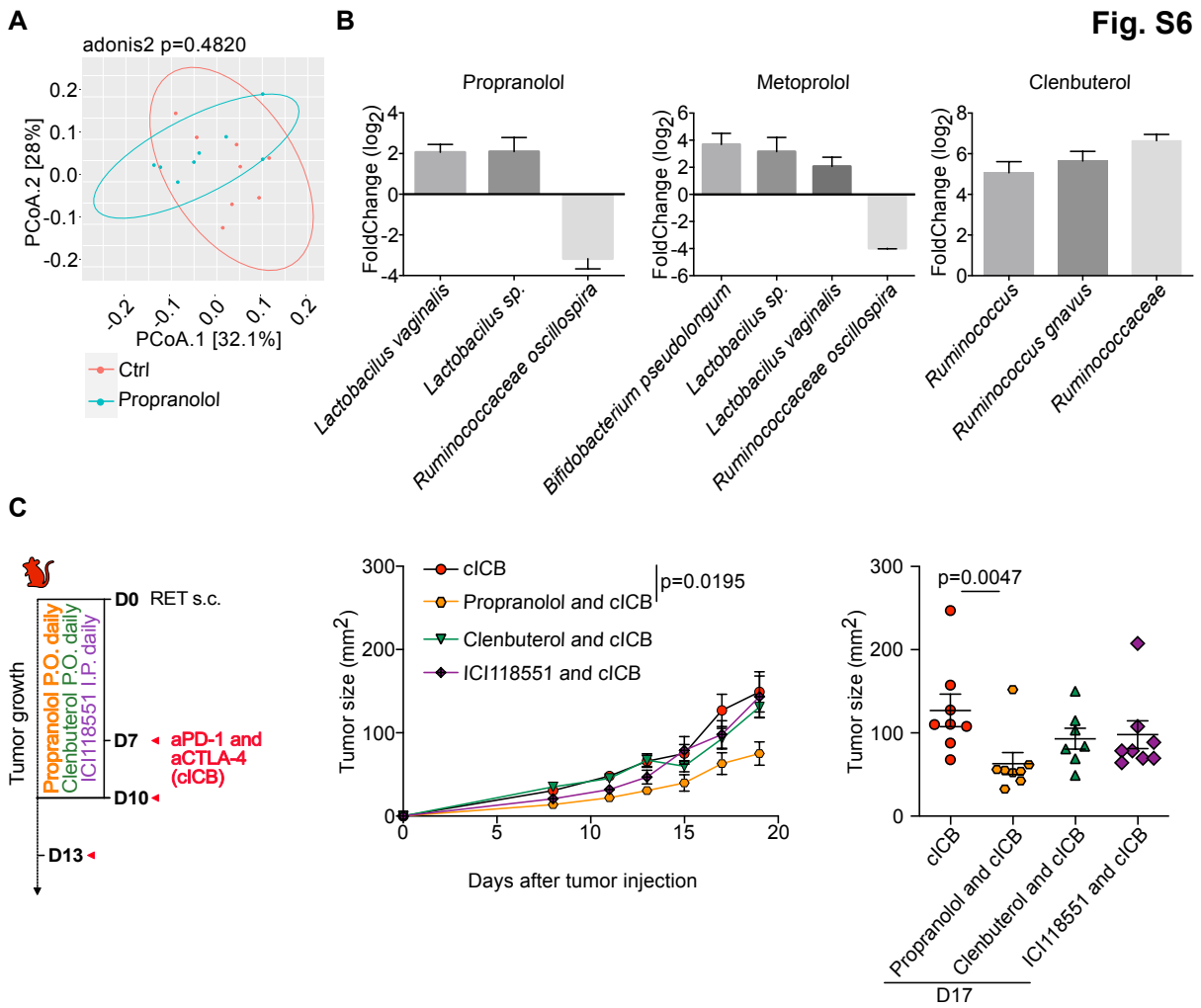
Fig. S6
A
adonis2 p=0.4820
PCoA.2 [28%]
PCoA.1 [32.1%]
Ctrl
Propranolol
B
Propranolol
Metoprolol
Clenbuterol
FoldChange (log2)
Lactobacilus vaginalis
Lactobacilus sp.
Ruminococcaceae oscillospira
Bifidobacterium pseudolongum
Ruminococcus
Ruminococcus gnavus
Ruminococcaceae
C
Tumor growth
D0 RET s.c.
Propranolol P.O. daily
Clenbuterol P.O. daily
ICI118551 I.P. daily
D7
aPD-1 and aCTLA-4 (cICB)
D10
D13
cICB
Propranolol and cICB
Clenbuterol and cICB
ICI118551 and cICB
p=0.0195
Tumor size (mm2)
Days after tumor injection
p=0.0047
D17

Supplemental Figure 6. Significant changes of the taxonomic composition of the stools after betablockade in RET tumor bearers.

A.Principal coordinate analysis of the changes of the taxonomic composition of feces (assessed by 16S rRNA sequencing of feces gene amplicons) during RET progression (day 7 *versus* day 0) in animals treated with PBS *versus* propranolol. ANOSIM and PERMANOVA define the separation of the groups; p values define the significance of group separation after 999 permutations of the samples. Each dot represents one stool. **B**. Significant differences depicted at the genus, family or species levels between propranolol or metoprolol (beta blockade) or clenbuterol (adrenergic receptor agonist) *versus* PBS-treated mice, as fold changes between pre- and post-RET inoculation at day 7 for 10 animals/group. Mann-Whitney test: Numerical p values are indicated. **C.** Refer to the experimental setting in Figure 6F (left). RET tumor growth kinetics overtime (middle), and cross-sectional assessment of tumor size at sacrifice (right) after a combination regimen composed of anti-PD-1 and anti-CTLA-4 Abs (cICB) and various pharmacological inhibitors or agonist of the sympathetic nervous system, depicted as mean±SEM of tumor sizes, over time or at sacrifice for 7-8 animals/group. A representative experiment out of 2 yielding similar conclusions is shown. Mann-Whitney test was used for comparison *versus* control group. ANOVA statistical analyses (Kruskal-Wallis test) were used for multiple comparison: Numerical p values are indicated.

Yonekura, Terrisse, Alves Costa Silva et al. Cancer induces a stress ileopathy depending on β-adrenergic receptors and promoting dysbiosis that contribute to carcinogenesis.

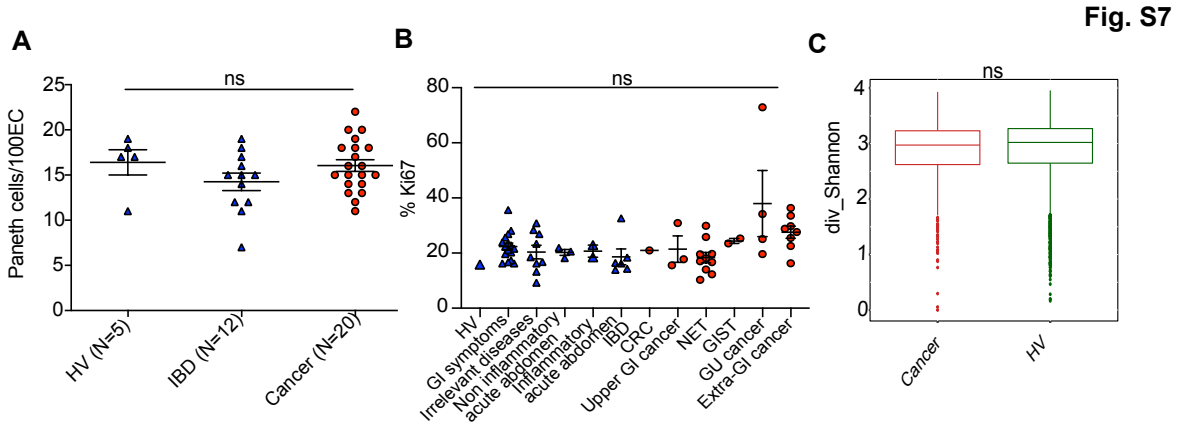

Supplemental Figure 7. Gut oncomicrobiome signature assessed by metagenomics analyses of cancer patient stools.

A.Immunohistochemistry hematoxylin/eosin/saffron staining to evaluate crypt Paneth cells in the ileum of patients suffering from colorectal cancer patients or inflammatory bowel disease or irrelevant disease (tumor free individuals without gastrointestinal tract related-disorders). Manual enumeration in 5 independent fields/individual, each dot representing one ileal tissue sample (biopsy or surgical resection)**. B.** Immunohistochemistry assessment of Ki67+ cells in the ileum of "healthy" cancer free volunteers (HV), patients suffering from colorectal cancers or cancers distant from the digestive tract (melanoma, ovarian cancer, kidney or bladder cancer, and Burkitt lymphoma) or inflammatory bowel disease or irrelevant diseases (tumor free individuals without gastrointestinal (GI) tract related-disorders). Also refer to Table S1 for description of patient characteristics, each dot representing one patient's sample. Statistical analyses by Mann-Whitney test *versus* HV: *ns:* not significant. GI: gastro-intestinal; IBD: Inflammatory bowel disease, CRC: colorectal cancer, NET: neuroendocrine tumors, GIST: gastrointestinal sarcoma, GU: genitourinary cancer. **C.** Richness of the taxonomic composition of feces from cancer patients compared to HV using the Shannon and Simpson index for 1637 stools from cancer patients across 8 malignancies and 5570 HV from the public data bases. NS: not significant**.**

Supplemental Table 1: Characteristics of patients from whom ileum specimen were used for histological analyses.

Supplemental Table 2: Characteristics of patients from whom serum samples were used for the quantification of soluble CD14 and soluble ST2.

Supplemental Table 3: Characteristics of patients from whom fecal samples were used for metagenomic analyses.